Results in Engineering 26 (2025) 105255

Contents lists available at ScienceDirect

Results in Engineering

journal homepage: www.sciencedirect.com/journal/results-in-engineering

Research paper

Reuse of P3HT:PCBM-based organic solar cells as photodetectors: Extending lifetime in optoelectronic applications

Fernando Rodríguez-Mas [a,*], Pablo Corral González [a], David Valiente García [b], Juan Carlos Ferrer Millán [b], José Luis Alonso Serrano [b]

[a] Communication Engineering Department, Miguel Hernández University, Elche, 03202, Spain
[b] University Institute for Engineering Research of Elche – I3E, Miguel Hernández University, Elche, 03202, Spain

ARTICLE INFO

Keywords:
OSCs
OPDs
Reuse
P3HT:PCBM
VLC
IoT

ABSTRACT

This study explores the reuse of organic solar cells at the end of their life cycle as organic photodetectors, promoting a sustainable model. Photodetectors were fabricated from organic solar cells using standard structures, and their characterization demonstrated technical feasibility as sensors/receivers in telecommunications applications. The results include a stable performance of the photodetector up to a frequency of 1000 kHz and a progressive reduction in voltage with transmission distance, with a significant drop at frequencies above 50 kHz, confirming its suitability for reliable data transmission in moderately noisy environments. These findings not only validate the use of repurposed organic photovoltaic devices as photodetectors but also highlight the positive impact on reducing electronic waste and extending the materials' lifetime. The photodetector's ability to operate in a self-powered mode underscores its potential for applications in energy-constrained environments. This approach represents progress towards a more sustainable energy model and it opens new opportunities for its implementation in sectors such as telecommunications, IoT, and advanced sensor systems.

1. Introduction

In the current context, renewable energy sources are key to achieve a sustainable energy model. Among them, solar energy stands out for its abundance and versatility. This article explores how organic solar cells (OSCs), beyond their role in energy generation, can be repurposed as organic photodetectors (OPDs) after reaching the end of their operational life, thereby fostering a more circular and sustainable economy.

1.1. The need for an energy transition towards renewable sources

The growth of the global population and industrialization have generated an unprecedented energy demand in recent decades [1]. This sustained increase in energy consumption has historically been associated with the exploitation of fossil fuels such as oil, coal, and natural gas, which constitute the majority of the primary energy used globally [2], Fig. 1. However, this energy model faces critical challenges that threaten global environmental [3], social [4], and economic stability [5]. In this context, the transition to renewable energy sources emerges not only as a viable alternative [6] but also as an imperative to ensure the planet's sustainability and the quality of life for future generations [7].

Reliance on fossil fuels has caused severe environmental consequences [9]. Human activities, particularly the burning of fossil fuels, have significantly increased greenhouse gas (GHG) concentrations in the atmosphere, with carbon dioxide (CO_2) being the primary contributor [10]. This phenomenon has led to an average rise in global temperatures [11], with secondary effects such as ocean acidification [12], biodiversity loss [13], and the intensification of extreme weather events [14]. Another drawback associated with the use of fossil fuels is their uneven geographical distribution [15]. Oil and natural gas reserves are concentrated in a limited number of regions, creating energy dependencies between importing and exporting countries. This dynamic generates geopolitical vulnerabilities, including international conflicts and energy price volatility, which affect the economic stability of entire nations [16].

The transition to renewable energy sources, Fig. 2, can significantly reduce this dependency by utilizing natural resources such as solar radiation, wind, water, and biomass, which are more evenly distributed across the planet [17]. Renewable energy sources, which rely on natu-

* Corresponding author.
E-mail address: fernando.rodriguezm@umh.es (F. Rodríguez-Mas).

https://doi.org/10.1016/j.rineng.2025.105255
Received 25 February 2025; Received in revised form 22 April 2025; Accepted 7 May 2025
Available online 13 May 2025

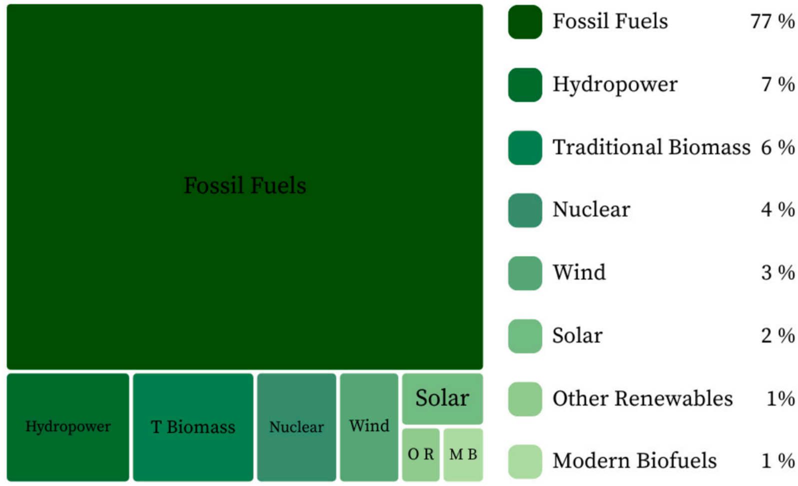

Fig. 1. Global primary energy consumption by source in 2021. Data from [8].

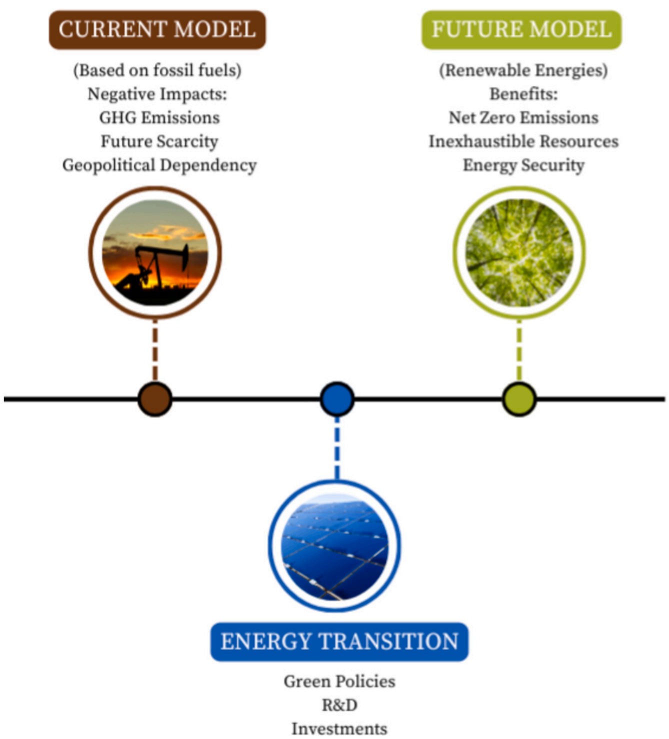

Fig. 2. Energy Transition Diagram.

ral flows such as sunlight and wind, are virtually inexhaustible. Their integration into energy systems ensures long-term energy availability.

In addition to environmental and strategic benefits, renewable energy offers significant opportunities for socioeconomic development [18]. The deployment of renewable technologies can promote job creation in sectors such as the installation, operation, and maintenance of energy infrastructure. According to the International Renewable Energy Agency (IRENA), the renewable energy sector increased job creation [19]. Moreover, renewable energy enables decentralized access to electricity, which is particularly relevant in remote and developing regions [20], where traditional electrical grids are limited or nonexistent. In order to recognize the risks associated with fossil fuels and the need for an energy transition, the international community has made ambitious commitments, like the Paris Agreement. The 2015 Paris Agreement is a key milestone in this context, setting the goal of limiting global warming to below 2 °C, with additional efforts not to exceed 1.5 °C [21]. Achieving this goal requires a drastic reduction in GHG emissions, where the widespread adoption of renewable technologies becomes crucial.

At the regional level, various initiatives are promoting policies that support renewable energy, such as tax incentives, subsidies, and favorable regulatory frameworks. These measures are essential to accelerate the adoption of these technologies, overcoming economic barriers, and stimulating investment in research and development [22]. In light of the environmental, economic, and social challenges associated with the current energy model, the transition to renewable energy sources is a global priority. This is not merely a technical or economic issue but a structural transformation that involves redefining the systems for energy production, distribution, and consumption.

1.2. Photovoltaic energy: a solution within renewables

Among the various renewable energy sources available, photovoltaic energy stands out as one of the most advantageous options due to its versatility, scalability, and virtually unlimited availability [23]. Unlike other renewable technologies, such as wind or hydropower, which rely on specific locations and particular climatic conditions, photovoltaic energy can be deployed across a wide range of environments, from residential rooftops and rural areas to large solar farms in deserts [24].

One of the greatest strengths of photovoltaic energy is its ability to directly convert sunlight into electricity through the photovoltaic effect, a process that generates no polluting emissions during operation. This positions it as a key technology in the transition towards a sustainable energy model, particularly in a context where electrification of sectors such as transportation and industry is essential to reduce GHG emissions [25].

The installation of photovoltaic panels is currently dominated by silicon-based technologies, which account for over 90% of global production [26]. Silicon, being abundant in the Earth's crust, is an economical and accessible material. Furthermore, its semiconductor properties make it ideal for solar cell manufacturing [27]. These characteristics have allowed the crystalline silicon-based solar industry to establish itself as the dominant technology, supported by a robust global production and supply infrastructure [26].

However, the predominance of silicon in the photovoltaic market presents certain challenges. The production of silicon solar cells involves energy-intensive and material-demanding processes, such as purifying silicon to ultra-high purity levels [28] and the production of ingots and wafers [29], Fig. 3.

Although these stages have been progressively optimized, their environmental impact remains significant [30]. Furthermore, it appears that the efficiencies of silicon solar panels are approaching their theoretical limit [31]. As the installation of photovoltaic panels continues to

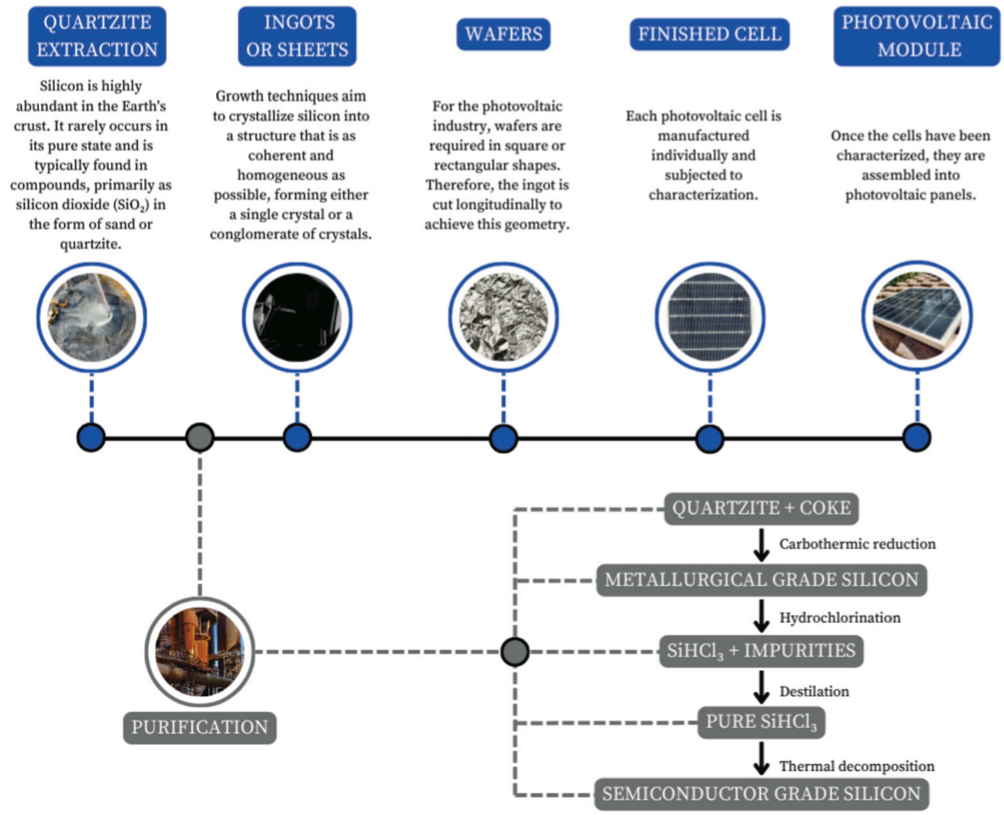

Fig. 3. Process of silicon purification and photovoltaic module fabrication. Data from [28].

expand, another relevant challenge associated with silicon-based technology is managing the end-of-life phase of panels. The average lifetime of a photovoltaic panel is estimated to range between 25 and 30 years [32], as a result, the first generations of large-scale installations are now reaching the decommissioning phase. This creates a growing need to develop efficient recycling systems to recover valuable materials, such as silicon and conductive metals, minimizing waste and closing the product life cycle loop.

1.3. Organic solar cells: an innovative and sustainable alternative

OSCs emerge as a promising alternative, thanks to their unique characteristics and a set of advantages that position them as an innovative option within the renewable energy sector. One of the most significant strengths of OSCs lies in their manufacturing process, which offers notable contrasts to silicon-based technologies. While silicon solar cells require complex processes and are highly energy-intensive [28], as previously discussed (e.g., purification of the material to ultra-high purity levels [28] or the production of ingots and wafers [29]), OSCs utilize much simpler and more sustainable techniques [33]. OSCs can be manufactured using printing [34] and coating processes [35,36], which operate at low temperatures [37] and do not require extreme vacuum conditions for material processing [38]. These techniques will allow the continuous production of large photovoltaic films on flexible substrates [39]. This not only significantly reduces energy consumption during production but also lowers manufacturing costs. Moreover, unlike silicon panels, which are typically rigid and require specific support structures for installation, OSCs can be fabricated on lightweight and flexible substrates [39], simplifying transportation, handling, and integration. Thanks to their flexible structure, these devices could be integrated into a wide range of surfaces and products, including solar windows [40], building facades [41], smart clothing [42], and portable electronic devices [43]. This adaptability to unconventional shapes and contexts allows organic technology to expand the reach of solar energy, addressing sectors where conventional technologies face limitations.

Despite the numerous advantages of OSCs, these technologies still face challenges that must be addressed before they can fully compete with silicon-based cells in terms of efficiency [44] or durability [45]. Nevertheless, their potential to become a more cost-effective and versatile alternative continues to generate considerable interest within the scientific community and the energy industry. Although OSCs have made remarkable progress in terms of efficiency, achieving values above 18% in laboratories [46], they still fall short of the commercial efficiencies of silicon cells. For OSCs to compete on a large scale, it is necessary not only to close this gap but also to ensure that these efficiencies can be maintained in mass-produced devices, where loss factors and variability are more significant [47].

Currently, OSCs are primarily in research and development phases. While they have shown significant progress in terms of efficiency and stability over the past decades [48,49], they have not yet reached a sufficient level of maturity for mass production and large-scale commercialization [49]. However, projections for OSCs are promising. Thanks to their less complex and more efficient manufacturing processes, it is expected that once the production of these cells is industrialized and standardized, associated costs will be significantly lower [50]. This could make them particularly attractive for emerging markets and specific applications where initial cost is a decisive factor. A major challenge for OSCs is their lifetime, which is currently significantly shorter than that of silicon-based cells. As previously mentioned, while silicon solar panels have an average lifetime between 25 to 30 years, OSCs tend to degrade more rapidly due to the susceptibility of organic materials to environmental factors such as humidity or oxygen [51]. This shorter lifetime translates into a need for more frequent replacements, potentially increasing long-term operational costs and reducing their competitiveness in applications where longevity is crucial. Nonetheless, researchers are developing strategies to improve the stability of organic materials and extend the devices' lifetime [52].

Although the limited lifetime may be seen as a disadvantage for conventional applications, it also opens the door to an innovative approach: disposable electronics [53]. This concept involves producing low-cost, short-lived devices designed specifically for temporary or limited-use applications. For instance, OSCs could be utilized in portable electronic devices, environmental sensors, disposable consumer products, or even in humanitarian aid campaigns in remote areas, where low-cost solar energy could have a significant impact. This approach would enhance the value of OSCs within a specific context.

Regarding the growing concerns about sustainability and electronic waste management, the concept of disposable electronics can be complemented by reuse and recycling strategies that maximize the value of materials and components at the end of their primary lifecycle. In this context, OSCs present a unique opportunity due to the versatile nature of their materials and their ability to perform alternative functions in secondary applications once they are no longer effective as solar energy generators.

The reuse of OSCs not only helps reduce electronic waste but also represents an innovative approach to extending the lifecycle of devices, aligning with the principles of a circular economy. Among potential reuse applications, notable examples include sensors and, particularly promising, photodetectors [54]. One of the most promising applications for reused OSCs is their transformation into photodetectors. These are technologies that convert light into electrical signals and have a wide range of applications in telecommunications, security, medicine, and science. OSCs, even after losing part of their efficiency for energy conversion, retain their ability to respond to different wavelengths of light. This makes them ideal for applications such as photodetectors, which can be used in optical communication systems, as receivers, where the precise reception of light signals is critical for data transmission.

1.4. OSC-based photodetectors: a key ally for IoT and light pulse communications

The use of reused OSCs as OPDs for light pulse communications emerges as a particularly compelling technological solution [55], especially in the context of the growing expansion of the Internet of Things (IoT) [56]. Implementing IoT requires a vast infrastructure of sensors [57,58] and devices that operate efficiently, cost-effectively, and sustainably [59]. In this scenario, reused OSCs stand out due to their unique features, including their ability to self-power using light [60], which eliminates the need for external energy sources and it significantly reduces installation costs and complexity. Light pulse communication, also known as visible light communication (VLC), offers a viable alternative to traditional radiofrequency (RF) technologies [61], which may encounter spectrum congestion and interference issues in environments densely populated with IoT devices. Within this conceptual framework, home automation emerges as an instrumental tool of significance to optimize energy efficiency [62], security [63] and quality of life [64]. In this regard, the introduction of the IoT paradigm in home automation management could be considered as an innovative initiative. Through the interconnection of residential devices and systems via the network, an intelligent administration of resources is facilitated, encompassing aspects such as lighting [65] and climate control [66,67].

According to El Shafee et al. [68], the functions that a smart home system must be capable of, include controlling the temperature and humidity of the house, motion detection, fire and smoke detection, door states (open/closed), light level, and video monitoring. Given this premise and considering the remarks made by Cvitić et al., it is anticipated that by the year 2025, there will be 75 billion IoT devices [69]. The increase in the number of connected sensors and devices can lead to a significant rise in energy demand, impacting not only the sustainability of IoT solutions but also posing challenges in terms of costs and environmental footprint. Energy efficiency must be a central consideration in the design and development of IoT-based home automation systems, seeking innovative solutions to minimize consumption without compromising functionality and the user experience. Despite the growing transition towards the use of renewable energy sources in contemporary society, the electricity generation matrix remains predominantly reliant on the utilization of fossil fuels, this phenomenon underscores the imperative for a more accelerated transition towards sustainable energy practices, considering the environmental impact and the significance of mitigating consumption associated with IoT infrastructure.

Beyond the energy challenges associated with the extensive deployment of IoT sensors and devices, the consideration of electromagnetic radiation generated by these devices is crucial. Despite potentially appearing as a minor issue in contrast to the substantial benefits that would arise from the full implementation of this technology, research suggests that specific animals relying on natural electromagnetic fields for orientation may experience adverse effects due to artificial electromagnetic fields [70]. Moreover, exposing animals to such electromagnetic fields has been linked to a decline in their health and disruptions in behavior [71,72].

But the effects of electromagnetic pollution derived from IoT communications not only focus on wildlife but also have harmful effects on humans. In an article published in 2018, Russell indicated that despite the potential for multiple benefits, 5G technology's operating wavelengths may be harmful to biological systems [73]. Marshall et al. also presented a correlation between successful treatment of autoimmune diseases and protection against electrosmog (electromagnetic pollution) [74].

Some of the discussed issues associated with IoT could be addressed by implementing VLC systems. Generally, VLC systems rely on transmitting signals using electromagnetic signals with wavelengths within the visible spectrum [75]. By operating at these wavelengths, this technology would mitigate the increase in electromagnetic pollution and would not cause interference or overload issues with other signals [76]. Besides, since the standardization of white LEDs for indoor lighting in residences [77], VLC systems have been progressively evolving [78,79]. In the realm of VLC, information is conveyed through the modulation of optical sources, such as LEDs and laser diodes (LDs), at a rate surpassing the persistence of the human eye [80]. The IEEE 802.15.7 standard for optical wireless communication (OWC) introduces variable pulse position modulation (VPPM) and on-off keying (OOK) for optical wireless personal area networks (OWPANs), providing mechanisms for dimming control. These modulation techniques are specifically outlined for a solitary light source across different physical layers [81]. This standard encompasses a broader array of optical wireless communication technologies and outlines the utilization of OWC within optical wireless personal area networks (OWPANs). It addresses various aspects, including network topologies, addressing, collision avoidance, acknowledgment, performance quality indication, dimming support, visibility support, colored status indication, and color stabilization. Within this investigation, OOK is implemented alongside Manchester code to ensure stable dimming support and mitigate the occurrence of flickering.

This article aims to fabricate an OSCs that, after reaching the end of its operational life as an energy generator, will be repurposed as an OPDs. The process of fabrication, reuse, and recycling of these devices is outlined in Fig. 4. By giving OSCs a second life as OPDs, not only the reuse of material is optimized, but also significant economic savings are also generated. Reuse reduces the need for manufacturing new devices from scratch, lowering production costs and associated waste. This approach promotes sustainability while it also enhances the economic viability of renewable technologies by extending component lifetimes and minimizing environmental impact.

2. Experimental section

2.1. Materials

The materials used in the fabrication of the device include a glass substrate coated with indium tin oxide (ITO). For the hole trans-

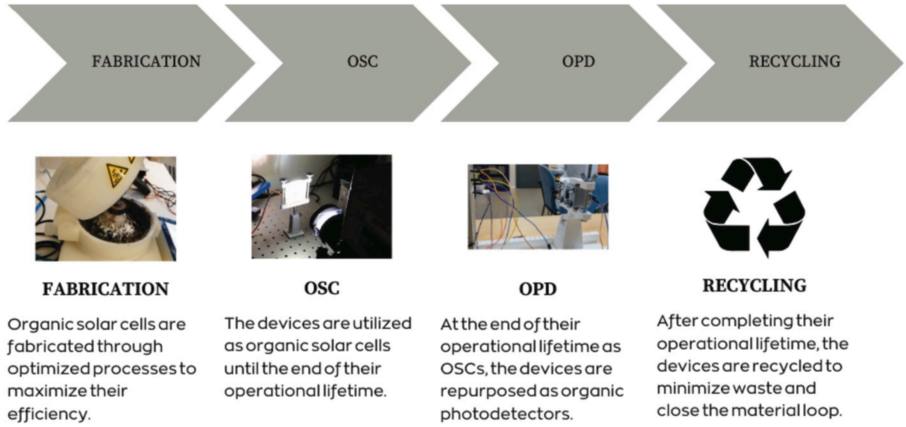

Fig. 4. Lifecycle, Reuse, and Recycling of Organic Optoelectronic Devices in Applications such as OSCs and OPDs.

port layer, poly(3,4-ethylenedioxythiophene) polystyrene sulfonate (PEDOT:PSS) in a 1.3% water solution was employed, while the active layer was fabricated using poly(3-hexylthiophene -2,5 - diyl) (P3HT) and (6,6)-phenyl-C_{61}-butyric acid methyl ester (PCBM). Regarding the solvents, chlorobenzene was used as the main solvent for preparing the active solution. Additionally, for the chemical bath, 1,2,4-trichlorobenzene, acetone, and isopropanol were used. All materials mentioned were purchased from Sigma-Aldrich and used without any additional purification.

2.2. Fabrication process of OSC

The possibility of repurposing OSCs as self-powered OPDs after the end of their photovoltaic lifetime presents an intriguing approach towards more sustainable and versatile devices. To demonstrate this feasibility, a solar cell with an ITO/PEDOT:PSS/P3HT:PCBM/Al structure was fabricated. The following sections detail the manufacturing process of this device, highlighting the most critical aspects of each phase. The process began with the preparation of substrates composed of glass coated with ITO. This material was selected for its transparency and conductivity, which are essential for its role as the anode in the solar cell. The substrates were cleaned using a sequence of ultrasonic baths in analytical-grade solvents: 1,2,4-trichlorobenzene, acetone, and isopropanol. This cleaning procedure effectively removed organic and inorganic residues, ensuring a contaminant-free surface. Subsequently, the substrates were dried using a flow of nitrogen gas (N_2).

Once the substrates were prepared, the hole transport layer was deposited using a PEDOT:PSS solution, widely recognized for its ability to enhance surface planarity and facilitate charge transport towards the electrode. The deposition was carried out via spin-coating, a technique that enables the formation of thin and uniform films. In this case, the spinning speed was set to 6000 rpm for 60 seconds, resulting in a uniform layer on the ITO surface. To improve the electrical properties of this layer and ensure adhesion, it was subjected to thermal annealing at 150 °C for 10 minutes.

The active layer, responsible for absorbing sunlight and generating electron-hole pairs, consisted of a blend of donor polymer (P3HT) and electron acceptor (PCBM) in a [1:0.8] ratio. The active solution was prepared by dissolving both components in a suitable organic solvent, followed by extended stirring to ensure homogeneity. The mixture was deposited on top of the PEDOT:PSS layer using the spin-coating technique, but at a lower speed of 300 rpm to produce a thicker layer with the desired morphology. Once formed, this layer underwent a drying process through heating at 150 °C for 10 minutes, allowing proper molecular organization within the active material, thereby enhancing charge transport within the cell.

Finally, the aluminum layer, which serves as the cathode, was deposited via thermal evaporation in a high-vacuum chamber. This process prevented metal oxidation and ensured the formation of a uniform film approximately 100 nm thick. A quartz crystal monitor was employed during this step to provide real-time control over the layer thickness, ensuring reproducibility of the procedure. The devices were encapsulated to protect them from environmental exposure.

2.3. Electrical characterization of the OSC

To evaluate the electrical properties of the fabricated OSC, Current Density-Voltage (J-V) measurements were performed under simulated illumination and in darkness. These measurements enabled the analysis of the photovoltaic performance of the cell and its potential for reuse as an OPD. The device configuration, based on the ITO/PEDOT:PSS/P3HT:PCBM/Al architecture, is illustrated in Fig. 5.

The initial electrical characterization was carried out under standard test conditions (AM 1.5G, 100 mW/cm^2) using a solar simulator equipped with a xenon lamp. Under these conditions, the current density and power/area versus voltage curves were obtained. The analysis also includes the spectral response in terms of external quantum efficiency (EQE) and evaluates the device's stability over time to determine its practical viability and potential for improvement.

The Fig. 5.A, which shows current density versus voltage, is fundamental for characterizing the electrical behavior of a photovoltaic device. This graph reveals two key parameters. First, the short-circuit current density (J_{sc}), which measures the amount of current generated by the device when the voltage is zero, has a value of 4.26 mA/cm^2, reflecting a significant capacity to generate current under standard illumination. Second, the open-circuit voltage (V_{oc}), representing the maximum voltage the device can produce in the absence of current flow, is 0.58 V. Additionally, the graph displays the characteristic shape of a diode, confirming the photoactive behavior of the evaluated device. The Fig. 5.B, which represents power generated per unit area versus voltage, provides key insights into the device's energy performance. The peak of the curve corresponds to the maximum power output, with a value of 1.29 mW/cm^2. Based on this value and considering an incident light intensity of 1000 W/m^2, the electrical efficiency was calculated to be 1.29%. Although this efficiency level is relatively low, it is sufficient to demonstrate the objective of this research: to give the device a second life once it has reached the end of its useful life as a photovoltaic device.

In Fig. 5.C, EQE as a function of wavelength, provides information about the device's spectral response. In this case, the EQE reaches its maximum value at a wavelength of 450 nm, indicating the device is most efficient in the blue region of the visible spectrum. This behavior can be attributed to the absorption properties of the active materials used, which exhibit a high absorption coefficient in this spectral region. However, as the wavelength increases towards 700 nm, the EQE decreases, likely due to limitations in the absorption properties of the active materials and carrier recombination losses in these spectral regions. Finally,

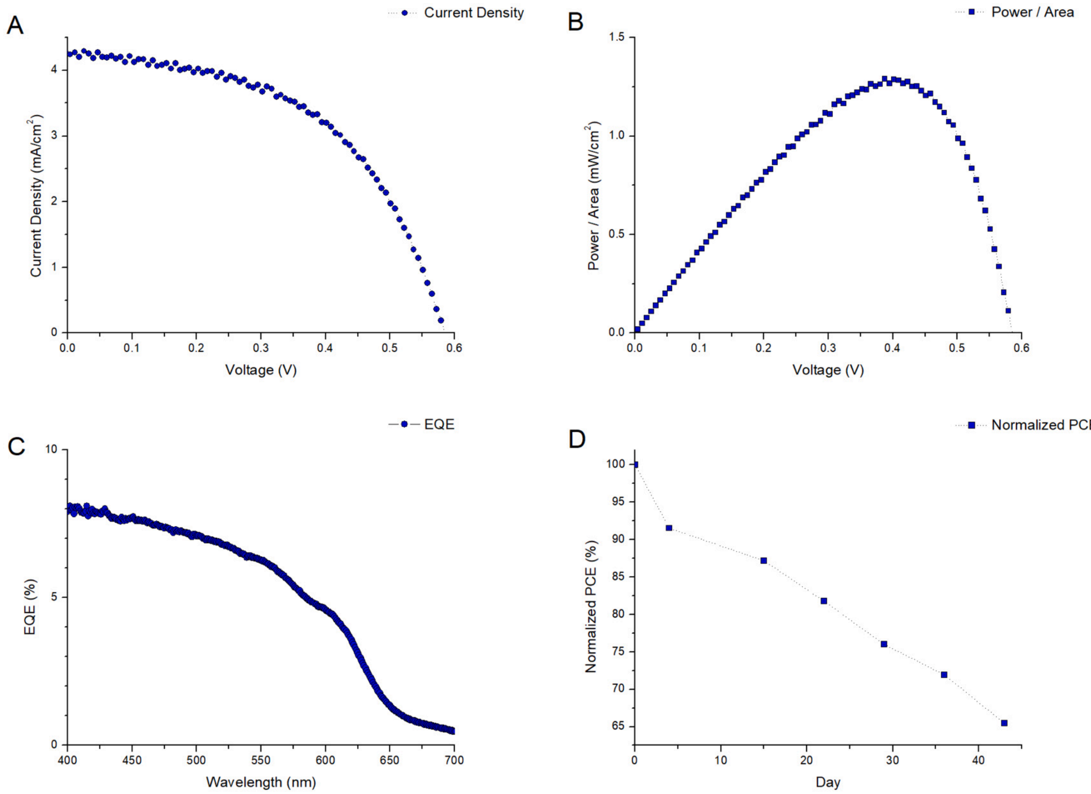

Fig. 5. Electrical and optical characterization of the device. (A) Current density versus voltage (J-V) curve. (B) Power per unit area as a function of voltage. (C) External Quantum Efficiency (EQE) spectrum. (D) Normalized Power Conversion Efficiency (PCE) as a function of time, showing the device's stability over 45 days.

Fig. 5.D, which illustrates normalized power conversion efficiency over time, evaluates the stability of the device. Stability is a critical factor in the development of photovoltaic technologies as it determines the practical viability of devices for commercial applications. In this case, the device initially retains 100% of its efficiency; however, after 12 days, it drops to 80%. This degradation pattern continues over time, reaching approximately 65% by the 40th day.

2.4. Proposal for a recycling process for OSCs

At the end of their service life, OSCs present both a challenge and an opportunity from an environmental and economic perspective. Proper management of these devices involves directing them to a recycling process that enables the recovery of valuable materials while reducing the environmental impact associated with their disposal. However, due to the limited commercialization of this type of device, there is currently no established recycling industry specific to OSCs. In the scientific literature, documented recycling processes for these cells focus primarily on recovering the glass substrate and ITO layer [82], materials that can be reused in the manufacture of new optoelectronic devices. Despite the absence of industrial infrastructure for recycling OSCs, it is possible to propose a theoretical process based on methodologies previously described and adapted to the specific characteristics of these cells. This procedure, designed to maximize the recovery of key materials while minimizing waste, could lay the groundwork for more sustainable and efficient recycling. The following sections describe a possible recycling process for OSCs with an ITO / PEDOT:PSS / P3HT:PCBM / Al structure, detailing the necessary steps for dismantling and separating each layer, Fig. 6.

The process begins with decapsulating the device, a critical step as OSCs are typically protected by glass adhered with a resilient epoxy. This encapsulation aims to preserve the integrity of internal layers from adverse environmental factors such as moisture and oxygen, which can degrade device performance. However, this protective barrier also complicates recycling, as the epoxy used must be carefully removed to avoid damaging the underlying materials. Several strategies are proposed to remove the protective glass and epoxy. One efficient technique involves applying controlled heat, raising the device temperature to a range of 100–150 °C. At these temperatures, the epoxy softens, facilitating the separation of the glass using precision tools. This method requires careful monitoring to avoid overheating, which could degrade the organic layers or substrate. Alternatively, specific solvents such as acetone or

Fig. 6. Proposal for a Recycling Process for OSCs.

isopropanol can dissolve the epoxy without significantly affecting the surrounding materials. While effective, this technique requires additional precautions in chemical handling and cleaning procedures to remove generated residues. In some cases, combining mechanical methods, such as manual scraping, with chemical techniques can optimize the decapsulation process and ensure exposure of the underlying aluminum electrode without compromising the integrity of the internal layers.

Once the device is decapsulated, the next step involves removing the aluminum electrode, which constitutes the outermost layer of the structure. This material is widely used in OSCs due to its low cost and high electrical conductivity, but recovering and reusing aluminum is crucial to minimize metal waste. The preferred approach for this stage is the use of chemical methods, applying mild acidic solutions such as diluted hydrochloric acid (HCl). This acid selectively dissolves the aluminum layer without affecting the internal layers of the cell. Subsequently, the dissolved aluminum can be recovered through techniques such as electrolysis, which allows the metal to precipitate in a solid and reusable form. This method not only ensures efficient material recovery but also minimizes the release of metallic waste into the environment.

To eliminate any remaining aluminum residues after chemical treatment, complementary mechanical methods, such as gentle scraping, can be employed. However, the use of such methods should be limited to avoid damaging the remaining functional layers.

The next stage focuses on removing the active layer, composed of a blend of conductive polymer (P3HT) and fullerene (PCBM). This layer is the functional core of OSCs, responsible for converting light into electrical energy. However, its complex composition requires specific techniques for separation and recovery. To dissolve this layer, organic solvents such as chloroform or toluene are used, as they are highly effective at breaking down the P3HT:PCBM blend without degrading the individual components. The resulting solution is then processed to separate and purify each component.

For instance, solvent evaporation yields solids corresponding to P3HT and PCBM, which can be purified using methods such as recrystallization or selective extraction. The recovery of these materials not only has economic value but also enables their reuse in the manufacture of new OSCs or other electronic applications. It is important to note that the use of organic solvents presents environmental and safety challenges, making it essential to implement solvent recycling practices and proper waste management to reduce the environmental impact of this stage.

After removing the active layer, the next step involves eliminating PEDOT:PSS, a conductive transparent polymer widely used in OSCs. This layer plays a crucial role in charge transport within the cell, but its recovery requires a different approach due to its water solubility. To dissolve this layer, deionized water or aqueous solutions adjusted to a specific pH are recommended to facilitate the removal of PEDOT:PSS. Applying ultrasonic waves during this process can be particularly useful for detaching the layer uniformly and efficiently. Once PEDOT:PSS is removed, the ITO substrate is cleaned using a diluted acetic acid bath or a similar agent, ensuring complete residue removal. This step prepares the substrate for reuse in the manufacture of new cells or electronic devices.

The final component to address in this process is the glass or plastic substrate coated with ITO, a critical material in OSCs due to its transparency and conductivity. Recovering the substrate with its ITO layer intact is essential, as it significantly reduces the production costs of new devices and promotes sustainability in the photovoltaic industry. Careful handling during the previous stages ensures that the substrate remains in optimal condition for reuse. Additionally, quality inspections can be implemented to identify defects or damage in the ITO layer, ensuring that the recycled material meets the required standards for future applications.

2.5. Reuse of OSC as OPD

At the end of their useful life as photovoltaic devices, OSCs could be given a second life by being repurposed as OPDs. This process takes advantage of the cell's residual ability to detect light rather than generate electrical energy, opening up new opportunities for reuse in sensor applications. By recycling OSCs in this way, not only their lifetime is extended, but it also contributes to sustainability by reducing electronic waste.

But how could an OSC function as an OPD? The ability of an OSC to function as an OPD is based on the fundamental principle of photovoltaic conversion. When illuminated by electromagnetic radiation, an OSC generates an electric current and voltage as a result of photon absorption. This process, known as the photovoltaic effect, is also the underlying mechanism of photodetector operation. While the primary operational purposes of these devices differ, both share the ability to interact with incident light and produce an electrical signal. In OSCs, the active material absorbs photons, generating electron-hole pairs that are separated under the influence of an internal electric field. This charge separation results in an electrical current that can be measured in an external circuit. The same mechanism enables an OSC to operate as an OPD, as the generated current is proportional to the intensity of the incident light, making it suitable for detecting variations in illumination conditions. Consequently, an OPD can be defined as a device that converts changes in light intensity into a measurable electrical signal, a capability inherently present in illuminated OSCs.

A particularly noteworthy feature of OSCs is their ability to operate in a self-powered mode, meaning they do not require an external energy source. This is achieved because the device generates the necessary current for its operation when exposed to light. In this mode, the electrical signal produced by the solar cell is directly derived from photon absorption and is influenced by factors such as the intensity of the incident radiation, the EQE of the active material, and the charge transport properties of the device. The capability to operate in a self-powered mode positions OSCs as an optimal solution for applications requiring simplicity, low cost, and energy autonomy. For instance, in VLC systems, OSCs can serve as self-powered OPDs, detecting modulated light signals and converting them into digital information without the need for additional energy sources or complex circuitry. The versatility of OSCs to function as self-powered OPDs not only broadens their range of applications but also establishes them as a highly efficient and sustainable alternative for optoelectronic systems, excelling in fields such as environmental sensing and optical telecommunications.

To evaluate the potential reuse of the OSC as an OPD, the device described in the previous section was used. This OSC was fabricated on November 3, 2022. Two years after its fabrication, it was electrically characterized by measuring its current density versus voltage curve, as illustrated in Fig. 7.

Fig. 7 presents the electrical characterization of an organic solar cell two years after its fabrication. In Subfig. 7.A, the J-V curve is shown, while Subfig. 7.B displays the power generated per unit area as a function of voltage. In Fig. 7.A, it can be observed that the J_{sc} reaches a value of 2.637 mA/cm^2, which is significantly lower than the initial value of 4.26 mA/cm^2 recorded in Fig. 5.A, observing a reduction of 38.09%. This decrease indicates a notable reduction in the device's ability to generate current under standard illumination. On the other hand, the V_{oc} in Fig. 7.A is 0.030 V, a drastically lower value compared to the 0.58 V initially observed in Fig. 5.A. This pronounced reduction in V_{oc} results in a significant decrease in the overall electrical performance of the device.

In Fig. 7.B, the graph of power generated per unit area as a function of voltage exhibits a peak value of 0.023 mW/cm^2, representing a 98.21% reduction compared to the 1.29 mW/cm^2 recorded in Fig. 5.B during the initial characterization of the device. This decline is consistent with the reductions observed in J_{sc} and V_{oc}, indicating a significant degradation in photovoltaic performance.

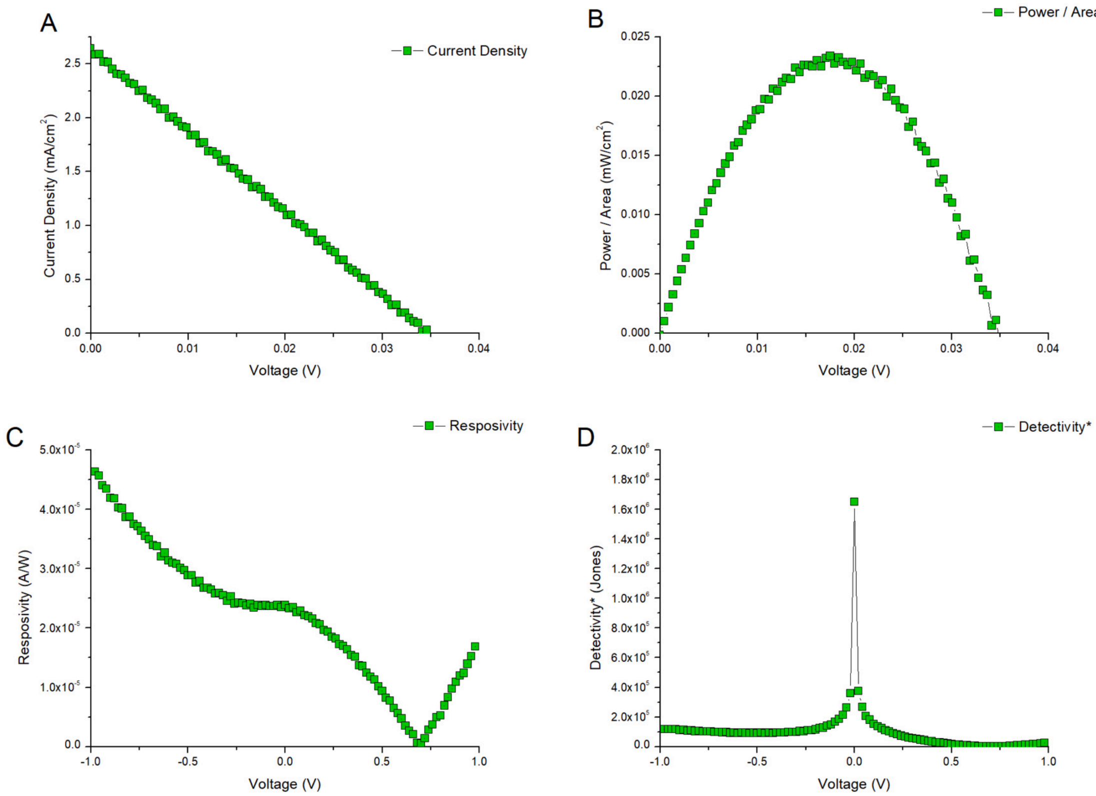

Fig. 7. Electrical characterization of the device two years after fabrication. (A) Current density versus voltage (J-V) curve. (B) Power per unit area as a function of voltage. (C) Responsivity (R) of the device under standard illumination conditions. (D) Specific detectivity (D*) of the device considering system noise and responsivity.

The current efficiency of the device is merely 0.023%, in contrast to the initial 1.29%. This substantial loss in performance can be attributed to the degradation of the organic materials used, as well as the inherent instability of this type of device under environmental conditions. The comparison between Figs. 5 and 7 confirms that, over the two years following its fabrication, the device has undergone considerable degradation in its electrical properties, significantly reducing its energy conversion capability.

In addition to the previously discussed electrical parameters, the responsivity and specific detectivity of the device were also analyzed. Fig. 7.C presents the responsivity (R), which represents the current generated per unit of incident light power. Under an irradiance of 100 mW/cm^2, the device exhibited a value of 2.4×10^{-5} A/W. On the other hand, Fig. 7.D shows the specific detectivity (D*), which considers both the responsivity and the system noise, yielding a value of $1.7 \times 10^6\ Jones$. Although these values are low, they may be suitable for applications that do not require high sensitivity, such as low-cost sensors or passive environmental monitoring systems.

To evaluate the performance of the OSC as an OPD, the following experimental setup was used:

The system was configured to determine the maximum frequency supported by a VLC system. In this setup, the transmitter consisted of a high-luminosity phosphor-based white LED with a correlated color temperature of 5500 K. An arbitrary waveform generator (AWG, Digilent® Analog Discovery 2) was used to generate signals, which were applied to the LED. The AWG operated with an analog bandwidth of 12 MHz and a sampling rate of 100 MSamples/s. The generated VLC signal was transmitted over a fixed distance and then detected by a self-powered OPD. The OPD was connected to a real-time oscilloscope (RTO, Digilent® Analog Discovery 2) for signal detection. The RTO had an analog bandwidth of 30 MHz and a sampling rate of 100 MSamples/s, ensuring precise detection and analysis of the signal, as illustrated in Fig. 8.

The Fig. 9 illustrates the relationship between voltage (in mV) and frequency (in kHz) across multiple distances, ranging from 0 cm to 20 cm, as indicated by distinct markers and colors in the legend. The data is presented in two panels, with the top graph serving as an inset of the bottom graph. Both panels display a similar overall trend, but the absolute voltage values differ significantly.

In the main graph (bottom panel), the maximum voltage is approximately 55 mV, observed at the lowest frequency (1 kHz) and the shortest distance (0 cm). As the frequency increases, the voltage decreases sharply, particularly for short distances. For distances beyond 3 cm, the voltage values converge at higher frequencies, stabilizing at low levels. Notably, shorter distances (0–3 cm) exhibit a clear differentiation in voltage responses, emphasizing a stronger dependence on distance at lower frequencies.

The inset graph (top panel) highlights the same trend at a smaller voltage range, with maximum values reaching approximately 20 mV at the lowest frequency (1 kHz) and the shortest distance (0 cm). Similar to the main graph, the voltage decreases with increasing frequency, though the reduction is less pronounced than in the main panel. The curves for larger distances exhibit minimal variation, underscoring the dominant influence of shorter distances at low frequencies.

In summary, the data demonstrates a strong dependence of voltage on both frequency and distance, with the highest voltage values occurring at low frequencies and short distances. The attenuation of voltage with increasing frequency and distance is evident in both panels, reflecting the diminishing effect of the measured phenomenon under these conditions.

The Fig. 10 presents the relationship between voltage (in mV) and distance (in cm) for various frequencies ranging from 1 kHz to 1000 kHz, as indicated by the distinct colors and markers in the legend. The data indicate a strong dependence of the voltage on both frequency and distance, with higher voltages observed at lower frequencies and shorter distances.

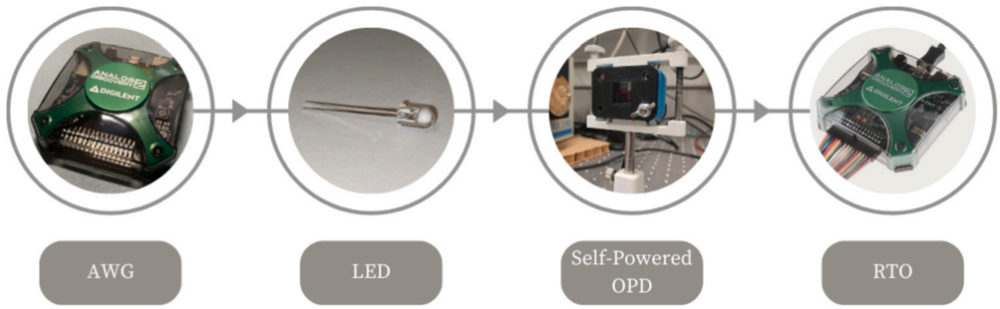

Fig. 8. Block diagram of the experimental setup, an arbitrary waveform generator, a high luminosity light-emitting diode, a self-powered OPD, and an RTO. AWG: Arbitrary waveform generator; RTO: Real-time oscilloscope. LED: Light-emitting diode, OPD: Organic photodetector.

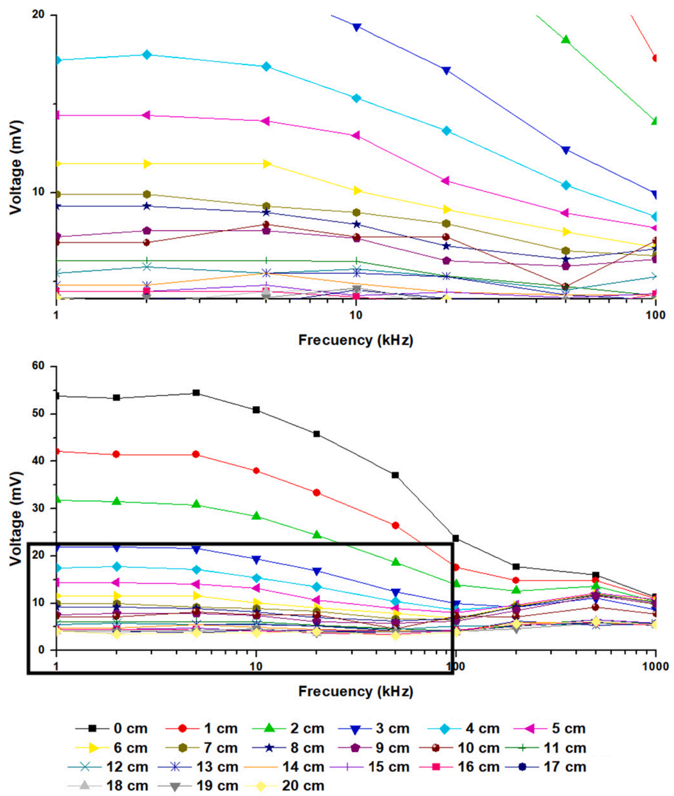

Fig. 9. Voltage as a function of frequency at different distances (0–20 cm). The main graph (bottom panel) shows the complete dataset, while the inset (top panel) highlights the same trend on a smaller voltage range. Both panels demonstrate a significant voltage decay with increasing frequency, particularly at shorter distances. Maximum voltage values are observed at the lowest frequency (1 kHz) and the shortest distance (0 cm).

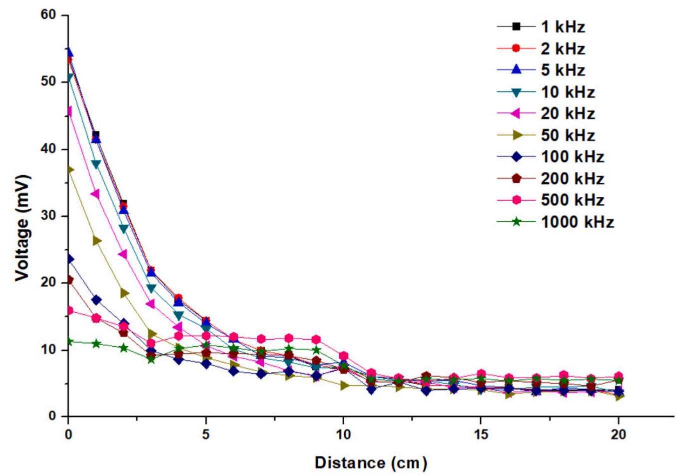

Fig. 10. Voltage as a function of distance for various frequencies (1 kHz–1000 kHz). The graph illustrates a rapid voltage decay with increasing distance, especially for lower frequencies (1, 2, and 5 kHz). Maximum voltage (≈55 mV) occurs at the shortest distance (0 cm) and the lowest frequency (1 kHz). Beyond 5 cm, the voltage stabilizes below 10 mV, with minimal differences between frequencies.

At the lowest frequency (1 kHz), the maximum voltage (≈55 mV) is recorded at the shortest distance (0 cm). As the distance increases, the voltage decreases sharply, particularly for low frequencies (1, 2, and 5 kHz). Beyond 5 cm, the voltage values for different frequencies start to converge, stabilizing at levels below 10 mV. This suggests that, at larger distances, the influence of frequency on voltage diminishes significantly. For higher frequencies (200, 500, and 1000 kHz), the voltage values are consistently lower across all distances and display less sensitivity to distance variations.

Overall, the data highlights the attenuation of the measured effect with increasing distance and frequency. The rapid voltage decay observed at short distances for low frequencies demonstrates the strong influence of these parameters, while at longer distances, the voltage stabilizes regardless of frequency.

Although the limited transmission range of OPDs might initially be perceived as a functional limitation, this characteristic endows them with significant potential for specific short-range applications, particularly in the interconnection of electronic devices within the IoT domain. One of the key technical advantages of OPDs is their self-powered capability, which eliminates the need for external energy sources, thereby reducing both the complexity of the systems and their energy consumption. In this context, OPDs can be employed to establish efficient communication channels between devices such as smartwatches, tablets, computers, and other electronic accessories. The restricted transmission distance is not a drawback but rather an advantageous feature for implementing compact, efficient systems that are free from electromagnetic interference. Furthermore, data transfer via encoded light signals provides a reliable communication method in environments with a high density of electronic devices.

Additionally, VLC systems with self-powered OPDs find prominent applications in the security domain. A representative implementation is their use in authentication systems based on physical proximity, such as access control terminals. In this case, a blinking light source transmits a unique code that is detected and deciphered by the OPD, enabling secure access validation. The ability to operate without requiring external power sources significantly simplifies installation and makes these systems viable in environments where additional energy infrastructure is complex or impractical.

In the logistics and smart packaging sector, this technology also finds relevant applications. OPDs can be integrated into electronic labeling systems, where a light-emitting source transmits encoded information

Table 1
Comparison between the repurposed organic photodetector and a commercial silicon photodiode (BPW21R, Vishay). Key parameters relevant for assessing their suitability in short-range optical communication applications.

Parameter	Repurposed Organic Photodetector	BPW21R Photodiode (Vishay)
Type	Organic photodetector	Silicon PN photodiode
Responsivity (A/W)	$\sim 2.4 \times 10^{-5}$	0.25 (at 565 nm)
Detectivity (Jones)	$\sim 1.65 \times 10^{6}$	$\sim 3.3 \times 10^{12}$
Dark current	~3.4 μA	2–30 nA (at 5 V reverse bias)
Active area	0.06 cm^2	0.075 cm^2
Bias range	+1 to −1 V	0 to −10 V

regarding traceability, expiration dates, or specific product characteristics. This information is captured by the photodetector at short distances, eliminating the need for battery-powered or externally powered sensors. This approach not only enhances system sustainability but also reduces operational costs and the environmental impact associated with these systems.

In the automotive sector, VLC systems can facilitate communication between internal electronic components of a vehicle. For instance, diagnostic modules and nearby sensors can exchange information via optical signals, replacing traditional physical or wireless connections in scenarios where these are less practical. The self-powered capability of OPDs contributes to a reduction in both the complexity and weight of the system, critical factors in modern vehicle design.

Finally, in controlled industrial environments, self-powered OPDs are particularly useful for communication between collaborative robots or automated machinery operating in proximity. The ability to transmit data using visible light at short distances is especially valuable in areas where electromagnetic interference poses an operational challenge. This approach ensures reliable and precise communication between system components, enhancing operational efficiency and safety.

In summary, these use cases exemplify how repurposed organic photodetectors can be functionally integrated into real-world applications, where their performance—while limited in absolute terms—is sufficient to meet specific operational requirements. Rather than competing directly with high-end photonic devices, their value lies in providing viable, sustainable, and low-cost solutions aligned with the principles of the circular economy.

To contextualize the performance of the developed photodetector, a comparison was conducted against a widely used commercial photodiode, the BPW21R from Vishay. Although the responsivity and detectivity values of the organic device are significantly lower, they are adequate for short-range optical communication applications, as discussed in the previous sections. Table 1 summarizes the key performance parameters.

Despite the numerical differences, experimental data demonstrate that the organic photodetector is capable of detecting optical signals at short distances and moderate frequencies, producing voltage responses of up to 55 mV at 1 kHz and 0 cm. This response progressively attenuates with increasing distance or frequency, aligning well with the requirements of systems where proximity and low power consumption are desired. These findings confirm the technical feasibility of repurposing end-of-life organic solar cells as self-powered photodetectors for visible light communication systems. This approach not only extends the operational life cycle of photovoltaic devices but also unlocks new opportunities for their integration into sectors that prioritize energy efficiency, system sustainability, compact design, and immunity to electromagnetic interference.

In this context, we propose a new perspective for the design and implementation of optoelectronic systems in emerging application scenarios, emphasizing the critical role that recycled organic photodetectors can play in the transition toward more sustainable and functionally adaptive electronics.

3. Conclusions

This study has demonstrated that OSCs, after completing their useful life as photovoltaic generators, can be repurposed as OPDs. This approach maximizes the utilization of employed materials, reduces environmental impact, and fosters a more sustainable and circular economic model.

From a technical perspective, the OPDs manufactured from repurposed OSCs have shown satisfactory performance in various characterization tests. The voltage-frequency graph evidences that the device maintains a stable response up to a frequency of 1000 kHz, indicating its capability to operate in VLC systems without significant signal degradation. This behavior positions it as a viable option for high-speed applications in telecommunications. The analysis of the voltage-distance graph at different frequencies shows that the voltage generated by the OPD progressively decreases with increasing distance from the transmitter. However, this reduction is more pronounced at frequencies above 50 kHz, suggesting the need to optimize the system design to ensure effective transmission in longer-distance environments. At lower frequencies, the device maintains a reliable signal up to a distance of 20 cm.

This result confirms the OPD's ability to provide robust data transmissions, even in scenarios with moderate noise levels, which is essential for critical applications in IoT and optical communications. These findings confirm the technical feasibility of repurposing OSCs as OPDs, highlighting their potential for practical applications in telecommunications and sensors. Moreover, the positive environmental impact derived from reducing electronic waste and extending the lifecycle of the materials used in their manufacture is underscored.

From an environmental and economic standpoint, the proposed reuse and recycling approach represents an effective solution to minimize waste and reduce the manufacturing costs associated with new devices. The OPDs' ability to operate in a self-powered mode, utilizing light as an energy source, underscores their suitability for applications in remote or energy-restricted environments. Finally, this study emphasizes the need for continued research to enhance the stability and efficiency of OSC-based OPDs, as well as the establishment of policies that promote the industrial implementation of these technologies. The use of these devices in communication systems, sensors, and IoT devices could represent a significant step towards a more sustainable integration of optoelectronic technologies across various industrial sectors.

CRediT authorship contribution statement

Fernando Rodríguez-Mas: Writing – review & editing, Writing – original draft, Visualization, Validation, Methodology, Investigation, Formal analysis, Data curation, Conceptualization. **Pablo Corral González:** Validation, Formal analysis, Data curation. **David Valiente García:** Methodology, Investigation, Formal analysis, Data curation. **Juan Carlos Ferrer Millán:** Validation, Methodology, Investigation, Funding acquisition. **José Luis Alonso Serrano:** Validation, Data curation.

Declaration of competing interest

The authors declare that they have no known competing financial interests or personal relationships that could have appeared to influence the work reported in this paper.

Acknowledgements

This work has been supported by project CIAICO/2023/193 (Conselleria d'Educació, Universitats i Ocupació, Generalitat Valenciana, Spain).

Data availability

No data was used for the research described in the article.

References

[1] N. Armaroli, V. Balzani, The future of energy supply: challenges and opportunities, Angew. Chem., Int. Ed. 46 (1–2) (2007) 52–66, https://doi.org/10.1002/anie.200602373.
[2] C. Zou, Q. Zhao, G. Zhang, B. Xiong, Energy revolution: from a fossil energy era to a new energy era, Nat. Gas. Ind. B 3 (1) (2016) 1–11, https://doi.org/10.1016/j.ngib.2016.02.001.
[3] J.P. Dorian, H.T. Franssen, D.R. Simbeck, Global challenges in energy, Energy Policy 34 (15) (2006) 1984–1991, https://doi.org/10.1016/j.enpol.2005.03.010.
[4] R. Polack, S. Wood, K.N. Smith, An analysis of fossil-fuel dependence in the United States with implications for community social work, Crit. Soc. Work 11 (3) (2010) 140–154, https://doi.org/10.22329/csw.v11i3.5837.
[5] G. Semieniuk, Fossil energy in economic growth: a study of the energy direction of technical change, 1950-2012, SWPS, https://doi.org/10.2139/ssrn.2795424, 2016.
[6] J.L.E. Antonia, V. Herzog, Timothy E. Lipman, D.M. Kammen, Renewable energy: a viable choice, Environ. Sci. Policy Sustain. Dev. 43 (10) (2001) 8–20, https://doi.org/10.1080/00139150109605150.
[7] X. Wang, D.A. Ali, W. Zhao, Urban energy transition and quality of life: a comprehensive statistical study on the nexus of wind clean energy adoption, job creation, and livability, Sustain. Cities Soc. 108 (2024) 105436, https://doi.org/10.1016/j.scs.2024.105436.
[8] V. Smil, Energy Transitions: Global and National Perspectives, Praeger, Santa Barbara, California, 2016.
[9] Y. Zhou, Y. Wang, Y. Wu, T. Wang, S. Wang, X. Zhou, M.I. Lodhi, N.A. Adam, M. Bilal, Transitioning to green energy: assessing environmental development and sustainability in the Saudi Arabia, in: Sustainable Futures, 2025, 100596.
[10] K.M. Omemen, M.O. Aldbbah, Climate change: key contributors and sustainable solutions, Int. J. Electr. Eng. Sustain. (2025) 10–27.
[11] T. Ashar, Y. Zhang, C. Yang, W. Xu, M. Zeeshan Ul Haq, H. Tahir, H.M.M. Abbas, Z. Wu, Rubber intercropping with arboreal and herbaceous species alleviated the global warming potential through the reduction of soil greenhouse gas emissions, Sci. Rep. 15 (1) (2025) 3196.
[12] R.E. Zeebe, J.C. Zachos, K. Caldeira, T. Tyrrell, Carbon emissions and acidification, Science 321 (5885) (2008) 51–52, https://doi.org/10.1126/science.1159124.
[13] K.R. Shivanna, Climate change and its impact on biodiversity and human welfare, Proc. Indian Natl. Sci. Acad. 88 (2) (2022) 160–171, https://doi.org/10.1007/s43538-022-00073-6.
[14] O. Angélil, D.A. Stone, M. Tadross, F. Tummon, M. Wehner, R. Knutti, Attribution of extreme weather to anthropogenic greenhouse gas emissions: sensitivity to spatial and temporal scales, Geophys. Res. Lett. 41 (6) (2014) 2150–2155, https://doi.org/10.1002/2014GL059234.
[15] T.I. Awan, S. Afsheen, A. Mushtaq, Carbon-free energy—free energy supply, in: Influence of Noble Metal Nanoparticles in Sustainable Energy Technologies, Springer, 2025, pp. 19–47.
[16] E. Dogan, M.T. Majeed, T. Luni, Analyzing the impacts of geopolitical risk and economic uncertainty on natural resources rents, Resour. Policy 72 (2021) 102056, https://doi.org/10.1016/j.resourpol.2021.102056.
[17] I. Overland, J. Juraev, R. Vakulchuk, Are renewable energy sources more evenly distributed than fossil fuels?, Renew. Energy 200 (2022) 379–386, https://doi.org/10.1016/j.renene.2022.09.046.
[18] S. Karytsas, D. Mendrinos, C. Karytsas, Measurement Methods of Socioeconomic Impacts of Renewable Energy Projects, IOP Conference Series: Earth and Environmental Science, vol. 410, IOP Publishing, 2020, p. 012087.
[19] I. IRENA, Renewable energy jobs: Status, prospects & policies, Tech. Rep., IRENA Working Paper, International Renewable Energy Agency (IRENA), Abu Dhabi, 2011.
[20] D.N. Karamov, P.V. Ilyushin, K.V. Suslov, Electrification of rural remote areas using renewable energy sources: literature review, Energies 15 (16) (2022) 5881, https://doi.org/10.3390/en15165881.
[21] D. Welsby, J. Price, S. Pye, P. Ekins, Unextractable fossil fuels in a 1.5° C world, Nature 597 (7875) (2021) 230–234, https://doi.org/10.1038/s41586-021-03821-8.
[22] Q. Li, A. Khan, M. Xu, C. Sun, The regulatory power of fiscal and monetary policies in driving renewable energy: the moderating influence of political stability in belt and road initiative countries, Environ. Impact. Asses. Rev. 110 (2025) 107653.
[23] R. Dallaev, T. Pisarenko, N. Papež, V. Holcman, Overview of the current state of flexible solar panels and photovoltaic materials, Materials 16 (17) (2023) 5839, https://doi.org/10.3390/ma16175839.
[24] Y. Wang, B. Liu, H. Peng, Y. Jiang, Locating the suitable large-scale solar farms in China's deserts with environmental considerations, Sci. Total Environ. 955 (2024) 176911, https://doi.org/10.1016/j.scitotenv.2024.176911.
[25] C. Breyer, S. Khalili, D. Bogdanov, Solar photovoltaic capacity demand for a sustainable transport sector to fulfil the Paris agreement by 2050, Prog. Photovolt. 27 (11) (2019) 978–989, https://doi.org/10.1002/pip.3114.
[26] M. Bošnjaković, Advance of sustainable energy materials: technology trends for silicon-based photovoltaic cells, Sustainability 16 (18) (2024) 7962, https://doi.org/10.3390/su16187962.
[27] W.U. Rehman, H. Wang, R.Z.A. Manj, W. Luo, J. Yang, When silicon materials meet natural sources: opportunities and challenges for low-cost lithium storage, Small 17 (9) (2021) 1904508, https://doi.org/10.1002/smll.201904508.
[28] S. Maldonado, The importance of new "sand-to-silicon" processes for the rapid future increase of photovoltaics, ACS Energy Lett. 5 (11) (2020) 3628–3632, https://doi.org/10.1021/acsenergylett.0c02100.
[29] Y. Yu, X. Bai, S. Li, J. Shi, L. Wang, F. Xi, W. Ma, R. Deng, Review of silicon recovery in the photovoltaic industry, in: Current Opinion in Green and Sustainable Chemistry, 2023, 100870.
[30] X. Pan, S. Li, Y. Li, P. Guo, X. Zhao, Y. Cai, Resource, characteristic, purification and application of quartz: a review, Miner. Eng. 183 (2022) 107600, https://doi.org/10.1016/j.mineng.2022.107600.
[31] Z. Sun, X. Chen, Y. He, J. Li, J. Wang, H. Yan, Y. Zhang, Toward efficiency limits of crystalline silicon solar cells: recent progress in high-efficiency silicon heterojunction solar cells, Adv. Energy Mater. 12 (23) (2022) 2200015, https://doi.org/10.1002/aenm.202200015.
[32] J.K. Daljit Singh, G. Molinari, J. Bui, B. Soltani, G.P. Rajarathnam, A. Abbas, Life cycle assessment of disposed and recycled end-of-life photovoltaic panels in Australia, Sustainability 13 (19) (2021) 11025, https://doi.org/10.3390/su131911025.
[33] F. Rodríguez-Mas, D. Valiente, J.C. Ferrer, J.L. Alonso, S.F. de Ávila, Towards a greener photovoltaic industry: enhancing efficiency, environmental sustainability and manufacturing costs through solvent optimization in organic solar cells, Heliyon 9 (12) (2023), https://doi.org/10.1016/j.heliyon.2023.e23099.
[34] Z. Xia, T. Cai, X. Li, Q. Zhang, J. Shuai, S. Liu, Recent progress of printing technologies for high-efficient organic solar cells, Catalysts 13 (1) (2023) 156, https://doi.org/10.3390/catal13010156.
[35] V. Vohra, N.T. Razali, R. Wahi, L. Ganzer, T. Virgili, A comparative study of low-cost coating processes for green & sustainable organic solar cell active layer manufacturing, Opt. Mater. X 13 (2022) 100127, https://doi.org/10.1016/j.omx.2021.100127.
[36] V.S. Rao, R. Cheruku, V.M. Krishna, B. Gireesha, K.M. Rao, M.A. Habila, S.S. Han, Enhancing solar cell efficiency: in-situ polymerization with cu2o@ cuo core-shell nanostars, Results Eng. 24 (2024) 103222.
[37] Y. Li, H. Liu, J. Wu, H. Tang, H. Wang, Q. Yang, Y. Fu, Z. Xie, Additive and high-temperature processing boost the photovoltaic performance of nonfullerene organic solar cells fabricated with blade coating and nonhalogenated solvents, ACS Appl. Mater. Interfaces 13 (8) (2021) 10239–10248, https://doi.org/10.1021/acsami.0c23035.
[38] F. Rodríguez-Mas, D. Valiente, P. Corral, J.L. Alonso, S. Fernández de Ávila, Impact of dimethylformamide, tetrahydrofuran, and dimethyl sulfoxide on bulk heterojunction organic solar cells' efficiency and environmental footprint, Adv. Energy Sustain. Res. 5 (10) (2024) 2400193, https://doi.org/10.1002/aesr.202400193.
[39] C. Liu, C. Xiao, C. Xie, W. Li, Flexible organic solar cells: materials, large-area fabrication techniques and potential applications, Nano Energy 89 (2021) 106399, https://doi.org/10.1016/j.nanoen.2021.106399.
[40] J.-J. Shen, Recently-explored top electrode materials for transparent organic solar cells, Synth. Met. 271 (2021) 116582, https://doi.org/10.1016/j.synthmet.2020.116582.
[41] E. Mirabi, F. Akrami Abarghuie, R. Arazi, Integration of buildings with third-generation photovoltaic solar cells: a review, Clean Energy 5 (3) (2021) 505–526, https://doi.org/10.1093/ce/zkab031.
[42] J. Wan, R. Zhang, Y. Li, Y. Li, Applications of organic solar cells in wearable electronics, Wearable Electron. 1 (2024) 26–40, https://doi.org/10.1016/j.wees.2024.03.001.
[43] J. De Chen, H.-M. Liu, H. Ren, Y.-F. Zhang, H.-Y. Hou, Y.-Q. Li, Z. Su, J.-X. Tang, Semitransparent organic solar cells with viewing-angle-independent Janus structural colors, Adv. Opt. Mater. 11 (1) (2023) 2201848, https://doi.org/10.1002/adom.202201848.
[44] K. Fukuda, K. Yu, T. Someya, The future of flexible organic solar cells, Adv. Energy Mater. 10 (25) (2020) 2000765, https://doi.org/10.1002/aenm.202000765.
[45] A. Machín, F. Márquez, Advancements in photovoltaic cell materials: silicon, organic, and perovskite solar cells, Materials 17 (5) (2024) 1165.
[46] K. Jin, Z. Xiao, L. Ding, et al., 18.69% pce from organic solar cells, J. Semicond. 42 (6) (2021) 060502, https://doi.org/10.1088/1674-4926/42/6/060502.
[47] A. Machín, F. Márquez, Advancements in photovoltaic cell materials: silicon, organic, and perovskite solar cells, Materials 17 (5) (2024) 1165, https://doi.org/10.3390/ma17051165.
[48] H. Hoppe, N.S. Sariciftci, Organic solar cells: an overview, J. Mater. Res. 19 (7) (2004) 1924–1945, https://doi.org/10.1557/JMR.2004.0252.
[49] P. Ding, D. Yang, S. Yang, Z. Ge, Stability of organic solar cells: toward commercial applications, Chem. Soc. Rev. 53 (5) (2024) 2350–2387, https://doi.org/10.1039/D3CS00492A.

[50] C.J. Brabec, J.A. Hauch, P. Schilinsky, C. Waldauf, Production aspects of organic photovoltaics and their impact on the commercialization of devices, Mater. Res. Soc. Bull. 30 (1) (2005) 50–52, https://doi.org/10.1557/mrs2005.10.
[51] N.A. Tegegne, L.T. Nchinda, T.P. Krüger, Progress toward stable organic solar cells, Adv. Opt. Mater. 13 (4) (2025) 2402257.
[52] N. Ahmad, J. Yuan, Y. Zou, One more step towards better stability of non-fullerene organic solar cells: advances, challenges, future perspective, and era of artificial intelligence, Energy Environ. Sci. (2025).
[53] Y.R. Panthi, Transient Optical and Electrical Phenomena in Organic Semiconductors: Insights into Fundamental Photophysics, Resistive Switching, and Emulation of Synaptic Plasticity, 2024.
[54] P. Corral, F. Rodríguez-Mas, J.L. Alonso, J.C. Ferrer, S. Fernandez de Avila, A low-cost ieee 802.15. 7 communication system based on organic photodetection for device-to-device connections, Sensors 20 (3) (2020) 714, https://doi.org/10.3390/s20030714.
[55] X. Han, C. Han, M. He, J. Han, H. Yu, J. Gou, J. Wang, Ultralow turn-on voltage organic upconversion devices for high-resolution imaging based on near-infrared homotandem photodetector, Laser Photonics Rev. (2025) 2401375.
[56] J. Ajayan, S. Sreejith, A. Ravindran, A. George, B. Mounika, Recent developments in organic photodetectors for future industrial applications: a review, Sens. Actuators A, Phys. (2025) 116459.
[57] R. Kumar, V. Venkatesan, R. Periyasamy, B. Rubini, O.P. Kumar, S. Vincent, et al., A novel cpw-fed flexible antenna with circular polarization for enhanced vehicular communication systems, Results Eng. 25 (2025) 104337.
[58] J. Han, W. Deng, F. Hu, S. Han, Z. Wang, Z. Fu, H. Zhou, H. Yu, J. Gou, J. Wang, 2d materials-based photodetectors with bi-directional responses in enabling intelligent optical sensing, Adv. Funct. Mater. (2025) 2423360.
[59] Z.H. Ali, H.A. Ali, Towards sustainable smart iot applications architectural elements and design: opportunities, challenges, and open directions, J. Supercomput. 77 (6) (2021) 5668–5725, https://doi.org/10.1007/s11227-020-03477-7.
[60] P. Corral, F. Rodriguez-Mas, G. De Scals, D. Valiente, J.C. Ferrer, S.F. de Avila, Improvements of organic photodetectors for vlc using a new active layer, focal lens, and a transimpedance amplifier, Elektron. Elektrotech. 28 (4) (2022) 48–54, https://doi.org/10.5755/j02.eie.31292.
[61] I. Siddique, M.Z. Awan, M.Y. Khan, A. Mazhar, Li-Fi the next generation of wireless communication through visible light communication (vlc) technology, Int. J. Sci. Res. Comput. Sci. Eng. Inf. Technol. 5 (1) (2019) 30–37, https://doi.org/10.32628/CSEIT1838108.
[62] D.-H. Lee, K.-S. Chung, Unsynchronized duty-cycle control for sensor based home automation networks, KSII Trans. Int. Inf. Syst. 6 (4) (2012) 1076–1089, https://doi.org/10.32628/CSEIT1838108.
[63] J. Van Hoof, H.S. Kort, P.G. Rutten, M.S.H. Duijnstee, Ageing-in-place with the use of ambient intelligence technology: perspectives of older users, Int. J. Med. Inform. 80 (5) (2011) 310–331, https://doi.org/10.1016/j.ijmedinf.2011.02.010.
[64] A. Poncela, F. Coslado, B. García, M. Fernández, J. Ariza, G. Peinado, C. Demetrio, F. Sandoval, Smart care home system: a platform for eAssistance, J. Ambient Intell. Humaniz. Comput. 10 (2019) 3997–4021, https://doi.org/10.1007/s12652-018-0979-9.
[65] H. Güneş, D. Akdaş, Web based, low cost and modular home automation system, Teh. Vjesn. 23 (2) (2016) 533–538, https://doi.org/10.17559/TV-20141029135313.
[66] S. Garg, A. Yadav, S. Jamloki, A. Sadana, K. Tharani, Iot based home automation, J. Inf. Optim. Sci. 41 (1) (2020) 261–271, https://doi.org/10.1080/02522667.2020.1721581.
[67] E.A. Metwally, M.R. Ismail, A.A. Farid, Development of an iot occupant-centric metrics: a systematic literature review, Results Eng. 23 (2024) 102614.
[68] A. El Shafee, K.A. Hamed, Towards a wifi based home automation system, Int. J. Comput. Electr. Eng. 4 (6) (2012) 803.
[69] I. Cvitić, D. Peraković, M. Periša, M. Krstić, B. Gupta, Analysis of iot concept applications: smart home perspective, in: International Conference on Future Access Enablers of Ubiquitous and Intelligent Infrastructures, Springer, 2021, pp. 167–180.
[70] U. Warnke, Bees, Birds and Mankind: Destroying Nature by "electrosmog", E. Oppenheimer and Sons, 2009.
[71] A. Balmori, Electromagnetic pollution from phone masts. Effects on wildlife, Pathophysiology 16 (2–3) (2009) 191–199, https://doi.org/10.1016/j.pathophys.2009.01.007.
[72] W. Löscher, G. Käs, Conspicuous behavioural abnormalities in a dairy cow herd near a tv and radio transmitting antenna, Prakt. Tierarzt 79 (1998) 437–444.
[73] C.L. Russell, 5 g wireless telecommunications expansion: public health and environmental implications, Environ. Res. 165 (2018) 484–495, https://doi.org/10.1016/j.envres.2018.01.016.
[74] T.G. Marshall, T.J.R. Heil, Electrosmog and autoimmune disease, Immunol. Res. 65 (1) (2017) 129–135, https://doi.org/10.1007/s12026-016-8825-7.
[75] M. Dimian, A.-M. Cailean, A. Done, S. Vlad, P. Andrei, Visible light communication sensors with adaptive hysteretic circuits for automotive applications, Physica B, Condens. Matter 549 (2018) 31–34, https://doi.org/10.1016/j.physb.2017.09.045.
[76] N. Chi, H. Haas, M. Kavehrad, T.D. Little, X.-L. Huang, Visible light communications: demand factors, benefits and opportunities [guest editorial], IEEE Wirel. Commun. 22 (2) (2015) 5–7, https://doi.org/10.1109/MWC.2015.7096278.
[77] J. Armstrong, Y.A. Sekercioglu, A. Neild, Visible light positioning: a roadmap for international standardization, IEEE Commun. Mag. 51 (12) (2013) 68–73, https://doi.org/10.1109/MCOM.2013.6685759.
[78] D. Karunatilaka, F. Zafar, V. Kalavally, R. Parthiban, Led based indoor visible light communications: state of the art, IEEE Commun. Surv. Tutor. 17 (3) (2015) 1649–1678, https://doi.org/10.1109/COMST.2015.2417576.
[79] C. He, C. Chen, A review of advanced transceiver technologies in visible light communications, Photonics 10 (2023) 648, https://doi.org/10.3390/photonics10060648.
[80] X. Ma, K. Lee, K. Lee, Appropriate modulation scheme for visible light communication systems considering illumination, Electron. Lett. 48 (18) (2012) 1137–1139, https://doi.org/10.1049/el.2012.2195.
[81] S. Yoon, K. Lee, J. Cha, V. Mariappan, K. Young, D. Woo, J. Kim, Ieee Standard for Local and Metropolitan Area Networks—Part 15.7: Short-Range Optical Wireless Communications, IEEE Std, 2019, pp. 1–407.
[82] M.T. Dang, P.-L.M. Brunner, J.D. Wuest, A green approach to organic thin-film electronic devices: recycling electrodes composed of indium tin oxide (ito), ACS Sustain. Chem. Eng. 2 (12) (2014) 2715–2721, https://doi.org/10.1021/sc500456p.